CrossMark

Outage Performance of the Mixed RF/FSO Relaying Channel in the Presence of Interference

**Milica I. Petkovic[1] · Aleksandra M. Cvetkovic[1] ·
Goran T. Djordjevic[1] · George K. Karagiannidis[2]**

Abstract We present novel closed-form expressions for the outage probability of the amplify-and-forward dual-hop semi-blind relaying channel, composed of mixed radio frequency (RF)/free space optical (FSO) links, while the relay is corrupted by both co-channel interferences and noise. The RF link is assumed to follow Nakagami-m distribution, while the FSO link is under the influence of atmospheric turbulence modelled by the Gamma–Gamma fading taking pointing errors into account. The analytical results are validated by Monte Carlo simulations. The obtained general expressions are simplified when RF link is noise-limited. The numerical results show the existence of the outage probability floor, which can be taken into account in the system design.

Keywords Free space optical systems (FSO) · Outage probability · Radio frequency (RF) · Relay systems

✉ Milica I. Petkovic
milica.petkovic@elfak.ni.ac.rs

Aleksandra M. Cvetkovic
aleksandra.cvetkovic@elfak.ni.ac.rs

Goran T. Djordjevic
goran@elfak.ni.ac.rs

George K. Karagiannidis
geokarag@auth.gr

[1] Faculty of Electronic Engineering, University of Nis, Aleksandra Medvedeva 14, Nis 18000, Serbia

[2] Department of Electrical and Computer Engineering, Aristotle University of Thessaloniki, Thessaloniki, Greece

1 Introduction

The mixed dual-hop amplify-and-forward (AF) relaying system, composed of the radio frequency (RF) and free space optical (FSO) links, was recently proposed in [1–3]. This mixed relay configuration was inspired by the concept of multiplexing, i.e. it makes possible multiplexing several RF users into a single FSO link. According to [2], a connectivity gap between a backbone network and last-mile access network can be resolved by using a high-speed FSO link for the last-mile. A subcarrier intensity modulation scheme (SIM) [4–6] is employed to convert the RF signal from the first hop to the optical signal for re-transmission, while it was assumed that there is no interference between the RF and the FSO hops, since they operate on completely different sets of frequencies. The FSO link in the second hop will cover the last mile and ensure no existence of fibre optics between the buildings, which provides similar bandwidth in saving economic resources [1–3]. Furthermore, the outage performance of the mixed dual-hop RF/FSO relay system with Rayleigh RF link and the Gamma–Gamma FSO link was studied in [1]. Besides outage probability, the error and capacity performance of a similar configuration, which takes the pointing errors at FSO link into account, were investigated in [2]. Under assumption that RF and FSO links are, respectively, subjected to Rayleigh fading and recently proposed M-distributed turbulence with pointing errors, closed form expression for the outage probability was derived in [3].

Inspired by these three works, in this paper, we study the RF/FSO relaying channel, where the RF link is assumed to follow the more general Nakagami-m fading model [7]. Beside the Gamma–Gamma atmospheric turbulence [8–11], we consider that the intensity fluctuations of the optical signal at the destination are also caused by pointing errors [12–15], which occur as the consequence of building sway due to thermal expansions, weak earthquakes and strong wind. We present novel accurate closed-form expressions for the outage probability for the practical case when RF link is corrupted by N multiple co-channel interferences (CCIs) and the additive white Gaussian noise (AWGN) at the relay. The analysis of CCIs influence on system performance is important, since CCIs occur as a result of the frequency re-using in RF systems or can be caused by cross-polarization discrimination [16, 17]. The general results are simplified in the case when the RF link is noise-limited (NL). As a special case, the system with the negligible pointing errors is also considered, and the outage probability expressions are reduced. For the special case of Rayleigh fading channels (fading severity parameter equal to one), the novel closed-form expression for the outage probability is reduced to the corresponding result reported in [1]. All analytical results are validated by Monte Carlo simulations.

The paper is organized as follows. Model of the system is described in Sect. 2, while closed-form expressions for the outage probability are derived in Sect. 3. Section 4 presents numerical and simulation results with appropriate comments, while some concluding remarks are given in Sect. 5.

2 System and Channel Model

Figure 1 presents the mixed dual-hop relay system in the presence of CCIs and AWGN at the relay node R. The model of independent identically distributed (i.i.d.) CCIs is used, because it corresponds to the two limiting cases of the system performance. The worst case is when the interferers are located near the cell edges closest to the observed user cell, and
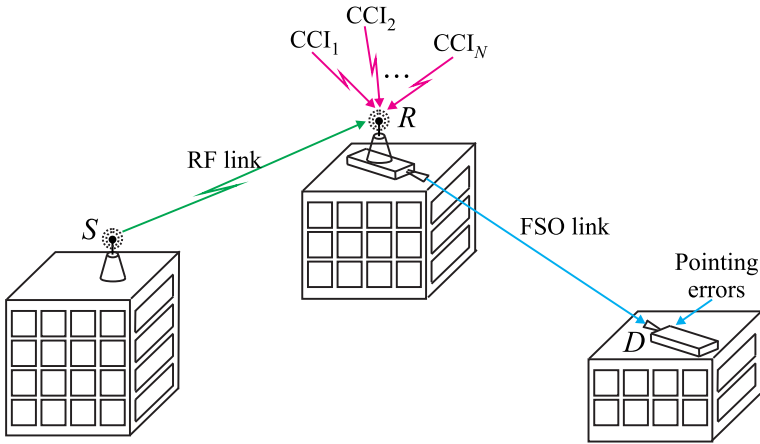
Fig. 1 System model of a mixed RF/FSO dual hop transmission system

the best case is when they are located near the farthest edges [16, 17]. The source node S communicates with the node R via the RF link, while the relay node R is connected with the destination node D via the FSO link. The electrical signal at the node R is converted to the optical one by SIM scheme.

The received signal at the relay is corrupted by N multiple CCIs, $\{r_i\}_{i=1}^{N}$, each with an average power of P_i. After removing the dc bias and an optical-to-electrical conversion, the received signal at the node D has the form

$$r_D = I_{RD} G \eta \left(h_{SR} r + \sum_{i=1}^{N} h_i r_i + n_{SR} \right) + n_{RD}, \tag{1}$$

where r is the RF signal transmitted from the node S with an average power P_s, h_{SR} is the desired signal fading amplitude over RF link, h_i is the i-th CCI fading amplitude, I_{RD} is the intensity of an optical signal at the node D, G is the relay gain, and η is an optical-to-electrical conversion constant. The level of the AWGN with zero mean and variance σ_{SR}^2 over RF link is denoted by n_{SR}, while the AWGN with zero mean and variance σ_{RD}^2 over the FSO link is denoted by n_{RD}. The thermal, background and dark current noise are all additive and independent [8, 18], so total noise of FSO hop is modelled as the AWGN which comprises all mentioned components.

Since the first RF hop is under the influence of Nakagami-m fading, the instantaneous signal-to-noise ratio (SNR) over the RF hop, $\gamma_1 = h_{SR}^2 P_S / \sigma_{SR}^2$, follows the Gamma distribution with probability density function (PDF) given by [7, Eq. (2.21)]

$$f_{\gamma 1}(\gamma_1) = \frac{m_1^{m_1}}{\Gamma(m_1)\mu_1^{m_1}} \gamma_1^{m_1-1} e^{-\frac{m_1 \gamma_1}{\mu_1}}, \tag{2}$$

where m_1 denotes the fading severity parameter, $\mu_1 = \mathrm{E}\left[h_{SR}^2 P_s / \sigma_{SR}^2\right]$ is the average SNR over the RF hop, and $\mathrm{E}[\cdot]$ denotes expectation. Since the interfering signals experience i.i.d. Nakagami-m fading, the total instantaneous interference-to-noise ratio (INR), $\gamma_I = \sum_{i=1}^{N} h_i^2 P_i / \sigma_{SR}^2$, follows also the Gamma distribution with parameters $N m_I$ and $N \mu_I$,

where m_I is the CCI fading severity parameter and $\mu_I = \mathrm{E}\left[h_i^2 P_i \big/ \sigma_{SR}^2\right]$ is the average INR per a CCI.

The relay gain can be defined similarly as in [19, 20] by

$$G^2 = \frac{P_t}{\mathrm{E}\left[h_{SR}^2\right]P_s + \sum_{i=1}^{N} \mathrm{E}\left[h_i^2\right]P_i + \sigma_{SR}^2} = \frac{P_t}{\sigma_{SR}^2 C_1}, \tag{3}$$

where P_t is the relay output signal power. The parameter $C_1 = P_t \big/ \left(\sigma_{SR}^2 G^2\right)$ can be found as

$$C_1 = \mu_1 + \mu_I N + 1. \tag{4}$$

Beside the Gamma–Gamma atmospheric turbulence, the second FSO hop is under the influence of pointing errors, so the intensity of an optical signal I_{RD} is described by the combined model with the PDF [14, Eq. (12)]

$$f_{I_{RD}}(I_{RD}) = \frac{\xi^2 \alpha \beta}{A_0 h_l \Gamma(\alpha)\Gamma(\beta)} G_{1,3}^{3,0}\left(\frac{\alpha\beta}{A_0 h_l} I_{RD} \middle| \begin{array}{ccc} & \xi^2 & \\ \xi^2 - 1, & \alpha - 1, & \beta - 1 \end{array}\right), \tag{5}$$

where $G_{p,q}^{m,n}(\cdot)$ denotes Meijer's G function defined by [21, Eq. (9.301)], α and β are atmospheric turbulence parameters, h_l is the attenuation due to atmospheric path loss and ξ and A_0 represent the parameters determined by pointing errors.

The parameters α and β represent the effective number of the small-scale and large scale cells. If the plane wave propagation and zero inner scale are assumed, the parameters α and β can be directly related with turbulence strength of FSO link as [8, p. 139, Eqs. (3.127), (3.128), 9, p. 511, Eq. (68)]

$$\begin{aligned} \alpha &= \left(\exp\left[\frac{0.49\sigma_R^2}{\left(1 + 1.11\sigma_R^{12/5}\right)^{7/6}}\right] - 1\right)^{-1}, \\ \beta &= \left(\exp\left[\frac{0.51\sigma_R^2}{\left(1 + 0.69\sigma_R^{12/5}\right)^{5/6}}\right] - 1\right)^{-1}, \end{aligned} \tag{6}$$

where σ_R^2 is the Rytov variance, defined as

$$\sigma_R^2 = 1.23 C_n^2 k^{7/6} L^{11/6}, \tag{7}$$

with the wave-number $k = 2\pi/\lambda$, the wavelength λ, the propagation distance L, and the refractive index C_n^2, which typically varies from 10^{-17} m$^{-2/3}$ to 10^{-13} m$^{-2/3}$ for weak to strong turbulence conditions, respectively.

The atmospheric conditions also have impact on the atmospheric path loss h_l, which is described by the exponential Beers-Lambert law as [12]

$$h_l = \exp(-\sigma L), \tag{8}$$

where σ denotes the atmospheric attenuation coefficient.

The pointing errors parameter ξ is defined as the ratio between the equivalent beam radius at the receiver, $w_{L_{eq}}$, and the pointing error (jitter) standard deviation, σ_s, at the receiver [12]

$$\xi = \frac{w_{L_{eq}}}{2\sigma_s}. \tag{9}$$

The equivalent beam radius at the receiver is dependent on the beam waist (radius calculated at e^{-2}) of a Gaussian beam propagation at distance L, w_L, and the radius of a circular detector aperture, a, as

$$w_{L_{eq}}^2 = \frac{w_L^2 \sqrt{\pi}\mathrm{erf}(v)}{2v\exp(-v^2)}, v = \frac{\sqrt{\pi}a}{\sqrt{2}w_L}. \tag{10}$$

The parameter A_0 denotes the fraction of the collected power at $L = 0$, defined as

$$A_0 = [\mathrm{erf}(v)]^2, \tag{11}$$

where erf(.) is the error function [21, Eq. (8.250.1)].

The optical beam waist at the receiver, w_L, can be related to optical beam waist at the output of transmitting laser, w_0, and radius of curvature, F_0, by [13]

$$w_L = w_0\sqrt{(\Theta_o + \Lambda_o)\left(1 + 1.63\sigma_R^{12/5}\Lambda_1\right)}, \tag{12}$$

where

$$\Theta_o = 1 - \frac{L}{F_0}, \Lambda_o = \frac{2L}{kw_0^2} \text{ and } \Lambda_1 = \frac{\Lambda_o}{\Theta_o^2 + \Lambda_o^2}. \tag{13}$$

Using (5), after some mathematical calculation and standard technique of transforming random variables, the PDF of the instantaneous SNR over the FSO hop, $\gamma_2 = \eta^2 I_{RD}^2 P_t^2 \big/ \sigma_{RD}^2$, is derived as

$$f_{\gamma_2}(\gamma_2) = \frac{\xi^2}{2\Gamma(\alpha)\Gamma(\beta)\gamma_2} G_{1,3}^{3,0}\left(\alpha\beta\varepsilon\sqrt{\frac{\gamma_2}{\mu_2}} \,\middle|\, \begin{matrix} \xi^2 + 1 \\ \xi^2, \quad \alpha, \quad \beta \end{matrix}\right), \tag{14}$$

where $\varepsilon = \xi^2 \big/ (\xi^2 + 1)$ and $\mu_2 = \eta^2 P_t^2 \mathrm{E}^2[I_{RD}] \big/ \sigma_{RD}^2$ represents the average electrical SNR over the FSO link, with $\mathrm{E}^2[I_{RD}] = \varepsilon^2 A_0^2 h_l^2$.

The greater misalignment between transmitter and receiver corresponds to less value of ξ, i.e. to greater values of σ_s and/or less value of w_0. Hence, when $\xi \to \infty$, it can be assumed that the intensity fluctuations of the received optical signal originate only from Gamma–Gamma atmospheric turbulence.

The overall signal-to-interference plus noise ratio (SINR) at the destination is given by

$$\gamma = \frac{\eta^2 I_{RD}^2 G^2 h_{SR}^2 P_s}{\eta^2 I_{RD}^2 G^2 \sum\limits_{i=1}^{N} h_i^2 P_i + \eta^2 I_{RD}^2 G^2 \sigma_{SR}^2 + \sigma_{RD}^2} = \frac{\gamma_1\gamma_2}{\gamma_2\gamma_I + \gamma_2 + C_1}. \tag{15}$$

In the case where the RF subsystem is NL, according to [1, Eq. (6)], the overall SNR at the destination can be expressed as

$$\gamma_{NL} = \frac{\eta^2 I_{RD}^2 G^2 h_{SR}^2 P_s}{\eta^2 I_{RD}^2 G^2 \sigma_{SR}^2 + \sigma_{RD}^2} = \frac{\gamma_1 \gamma_2}{\gamma_2 + C_2}, \tag{16}$$

where parameter C_2 is constant determined by the relay gain. When NL system is under investigation, the gain is defined as [20, Eq. (6)]

$$G_{NL}^2 = \frac{P_t}{\mathrm{E}\left[h_{SR}^2\right] P_s + \sigma_{SR}^2} = \frac{P_t}{\sigma_{SR}^2 C_2}, \tag{17}$$

so the parameter C_2 is found as

$$C_2 = \mu_1 + 1. \tag{18}$$

3 Outage Probability Analysis

The outage probability is the probability that the instantaneous end-to-end SINR, γ, falls below a predetermined protection ratio, γ_{th} [7]. For the system under the investigation, it can be written as

$$
\begin{aligned}
P_{out} &= \mathrm{Pr}\left[\frac{\gamma_1 \gamma_2}{\gamma_2 \gamma_I + \gamma_2 + C_1} < \gamma_{th}\right] \\
&= \int_0^\infty \int_0^\infty \mathrm{Pr}\left[\gamma_1 < \gamma_{th}\left(\gamma_I + 1 + \frac{C_1}{\gamma_2}\right)\right] f_{\gamma_2}(\gamma_2) f_{\gamma_I}(\gamma_I) d\gamma_2 d\gamma_I.
\end{aligned}
\tag{19}
$$

where Pr[.] denotes probability.

Using the cumulative distribution function (CDF) of the Gamma distribution [7, Table (9.5)], and applying [21, Eq. (1.111), 22, Eq. (06.06.06.0005.01)], after some mathematical manipulations (19) can be re-written as

$$
\begin{aligned}
P_{out} =\ & 1 - \sum_{k=0}^{m_1-1} \sum_{i=0}^{k} \binom{k}{i} \left(\frac{m_I}{\mu_I}\right)^{m_I N} \left(\frac{m_1 \gamma_{th}}{\mu_1}\right)^k \frac{\xi^2 C_1{}^i}{k! 2 \Gamma(\alpha) \Gamma(\beta) \Gamma(m_I N)} e^{-\frac{m_1 \gamma_{th}}{\mu_1}} \\
& \times \int_0^\infty \int_0^\infty \gamma_2^{-i-1} e^{-\frac{m_1 \gamma_{th} C_1}{\mu_1 \gamma_2}} G_{1,3}^{3,0}\left(\alpha\beta\varepsilon\sqrt{\frac{\gamma_2}{\mu_2}} \,\middle|\, \begin{matrix} \xi^2 + 1 \\ \xi^2, \ \alpha, \ \beta \end{matrix}\right) \\
& \times \gamma_I{}^{m_I N - 1} e^{-\gamma_I \left(\frac{m_1}{\mu_1}\gamma_{th} + \frac{m_I}{\mu_I}\right)} (\gamma_I + 1)^{k-i} d\gamma_2 d\gamma_I.
\end{aligned}
\tag{20}
$$

After applying the procedure described in Appendix A, the outage probability when relay suffers from the multiple CCIs and AWGN is derived in the closed-form given by

$$
\begin{aligned}
P_{out} =\ & 1 - \frac{2^{\alpha+\beta-3}\xi^2}{\pi\Gamma(\alpha)\Gamma(\beta)} \left(\frac{m_I}{\mu_I}\right)^{m_I N} e^{-\frac{m_1 \gamma_{th}}{\mu_1}} \sum_{k=0}^{m_1-1} \sum_{i=0}^{k} \binom{k}{i} \frac{1}{k!} \left(\frac{m_1 \gamma_{th}}{\mu_1}\right)^{k-i} \\
& \times \mathrm{U}\left(m_I N, k-i+m_I N+1; \frac{m_I}{\mu_I} + \frac{m_1 \gamma_{th}}{\mu_1}\right) G_{1,6}^{6,0}\left(\frac{\alpha^2 \beta^2 \varepsilon^2 m_1 \gamma_{th} C_1}{16 \mu_1 \mu_2} \,\middle|\, \begin{matrix} \frac{\xi^2+2}{2} \\ \kappa_1 \end{matrix}\right),
\end{aligned}
\tag{21}
$$

where $U(\cdot)$ is the confluent hypergeometric function defined by [21, Eq. (9.211.4)] and

$$\kappa_1 = \frac{\xi^2}{2}, \quad \frac{\alpha}{2}, \quad \frac{\alpha+1}{2}, \quad \frac{\beta}{2}, \quad \frac{\beta+1}{2}, \quad i. \tag{22}$$

If the pointing errors effect is negligible small, i.e. the intensity fluctuations of the optical signal at the node D are caused only by the Gamma–Gamma atmospheric turbulence, the instantaneous SNR over the FSO link, γ_2, has the PDF given by [1, Eq. (8)]. The outage probability of the system when pointing errors are neglected, can be derived by substituting [1, Eq. (8)] instead (14) into (19) by following similar derivation as in Appendix A. Another method implies considering $\xi \to \infty$ in (21) [3], which is presented in Appendix B. The outage probability of the system without pointing errors is derived as

$$
\begin{aligned}
P_{out,GG} = \lim_{\xi \to \infty} P_{out} = 1 &- \frac{2^{\alpha+\beta-2}}{\pi\Gamma(\alpha)\Gamma(\beta)} \left(\frac{m_I}{\mu_I}\right)^{m_I N} e^{-\frac{m_1 \gamma_{th}}{\mu_1}} \\
&\times \sum_{k=0}^{m_1-1} \sum_{i=0}^{k} \binom{k}{i} \frac{1}{k!} \left(\frac{m_1 \gamma_{th}}{\mu_1}\right)^{k-i} \\
&\times U\left(m_I N, k-i+m_I N+1; \frac{m_I}{\mu_I} + \frac{m_1 \gamma_{th}}{\mu_1}\right) G_{0,5}^{5,0}\left(\frac{\alpha^2 \beta^2 m_1 \gamma_{th} C_1}{16\mu_1\mu_2}\middle| \begin{matrix} - \\ \kappa_2 \end{matrix}\right),
\end{aligned}
\tag{23}
$$

with

$$\kappa_2 = \frac{\alpha}{2}, \quad \frac{\alpha+1}{2}, \quad \frac{\beta}{2}, \quad \frac{\beta+1}{2}, \quad i. \tag{24}$$

The outage probability of the relaying system with the NL RF link can be found as [1, Eq. (9)]

$$P_{out}^{NL} = \int_0^\infty \Pr\left[\gamma_1 < \frac{\gamma_{th}(\gamma_2 + C_2)}{\gamma_2}\right] f_{\gamma_2}(\gamma_2) d\gamma_2, \tag{25}$$

or by setting $N = 0$ into (21). After applying [22, Eq. (07.33.03.0013.01)] in (21), the outage probability is expressed as

$$
\begin{aligned}
P_{out}^{NL} = 1 &- \frac{2^{\alpha+\beta-3}\xi^2 e^{-\frac{m_1 \gamma_{th}}{\mu_1}}}{\pi\Gamma(\alpha)\Gamma(\beta)} \sum_{k=0}^{m_1-1} \sum_{i=0}^{k} \binom{k}{i} \frac{1}{k!} \left(\frac{m_1 \gamma_{th}}{\mu_1}\right)^{k-i} \\
&\times G_{1,6}^{6,0}\left(\frac{\alpha^2 \beta^2 \varepsilon^2 m_1 \gamma_{th} C_2}{16\mu_1\mu_2}\middle| \begin{matrix} \frac{\xi^2+2}{2} \\ \kappa_1 \end{matrix}\right),
\end{aligned}
\tag{26}
$$

where parameter C_2 is given by (18) and κ_1 is defied by (22).

For the system without pointing errors, the outage probability expression is derived by considering $\xi \to \infty$ in (26) and using similar approach as in Appendix B:

$$P_{out,GG}^{NL} = 1 - \frac{2^{\alpha+\beta-2}e^{-\frac{m_1\gamma_{th}}{\mu_1}}}{\pi\Gamma(\alpha)\Gamma(\beta)} \sum_{k=0}^{m_1-1} \sum_{i=0}^{k} \binom{k}{i} \frac{1}{k!} \left(\frac{m_1\gamma_{th}}{\mu_1}\right)^{k-i}$$
$$\times G_{0,5}^{5,0}\left(\frac{\alpha^2\beta^2 m_1\gamma_{th}C_2}{16\mu_1\mu_2} \middle| \begin{array}{c} - \\ \kappa_2 \end{array}\right). \tag{27}$$

If the RF link follows Rayleigh distribution (which is the special case of Nakagami-m distribution when $m_1 = 1$), then the observed relaying channel comes to that from [1]. It is verified that substituting $m_1 = 1$ in (27) and applying [22, Eq. (07.34.16.0001.01)] leads to [1, Eq. (15)].

4 Numerical Results

Novel outage probability expressions in (21), (23), (26) and (27) are given in terms of Meijer's G functions that are built in software package Mathematica 10 and can be efficiently numerically evaluated. Using [22, Eq. (07.34.26.0004.01)], Meijer's G function can be presented in terms of more familiar generalized hypergeometric functions denoted by $_pF_q(a_1, a_2, \ldots, a_p; b_1, b_2, \ldots, b_q; z)$ [21, Eq. (9.100^7)]. After some mathematical manipulations (21), (23), (26) and (27) can be presented in the equivalent forms in terms of the generalized hypergemetric functions that are not presented here because of the space limitations. In that case, $a_1, a_2, \ldots, a_p, b_1, b_2, \ldots, b_q$, should be $\neq -n, (n = 0, 1, 2, \ldots)$ since the generalized hypergeometric function has poles in these points. However, this is not inconvenience in practice because parameters α, β and ξ previously defined are not integers with high probability. In the case that any a_i or b_j ($i = 1, 2, \ldots, p; j = 1, 2, \ldots q$) is negative integer, the numerical value of generalized hypergeometric function could be evaluated for $a_i + \varepsilon$ and $b_j + \varepsilon$, where $\varepsilon = 10^{-4}$, instead of a_i and b_j, respectively. In contrast to this, even when α, β and ξ are integers, numerical values of outage probability can be evaluated in software package Mathematica 10 using derived Eqs. (21), (23), (26) and (27) containing Meijer's G functions, since this software package has very efficient algorithms for numerical evaluation of Meijer's G functions allowing symbolic evaluation of [21, Eq. (9.301)] including necessary reduction of expressions in numerator and denominator. Numerical results are validated by Monte Carlo simulations performed using software package Matlab 2013.

The results were obtained for the turbulence parameters α and β defined by (6) and (7), which are dependent on several physical parameters, such as: refractive index C_n^2, the wavelength $\lambda = 1550$ nm and the propagation distance $L = 1000$ m. The refractive index determines the turbulence strength in the following way: $C_n^2 = 6 \times 10^{-15}$ m$^{-2/3}$ for weak , $C_n^2 = 2 \times 10^{-14}$ m$^{-2/3}$ for moderate and $C_n^2 = 5 \times 10^{-14}$ m$^{-2/3}$ for strong turbulence conditions [23]. It should be noted that pointing errors parameter, ξ, is dependent on jitter standard deviation, σ_s, the radius of a circular detector aperture, $a = 5$ cm, radius of curvature, $F_0 = -10$ m, as well as other parameters such as C_n^2, λ, L and the optical beam waist at the output of transmitting laser, w_0.

Figure 2 presents the outage probability dependence on the average electrical SNR over the FSO link for different values of μ_1 and the jitter standard deviation σ_s in the case when the relay is corrupted only by noise. As expected, outage probability has lower values for greater values of μ_1. The greater values of parameter σ_s (corresponding to lower values of parameter ξ, see Eq. (9), and greater misalignment between transmitter and the receiver)
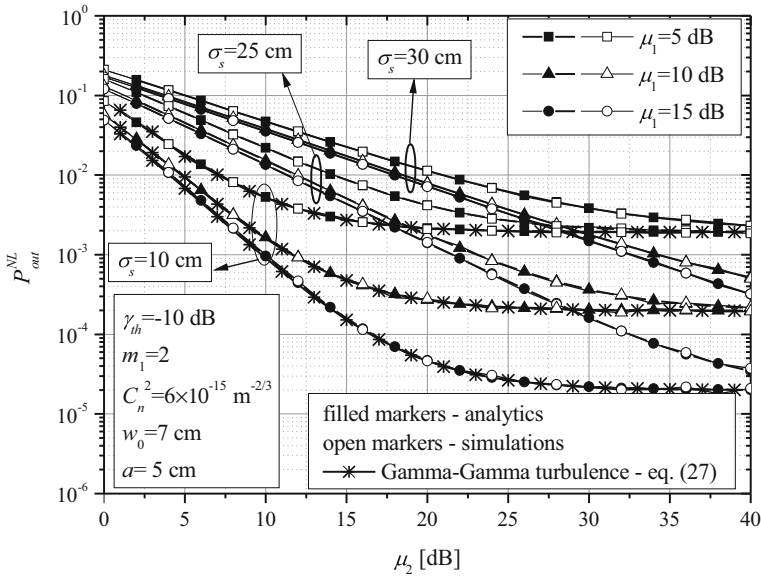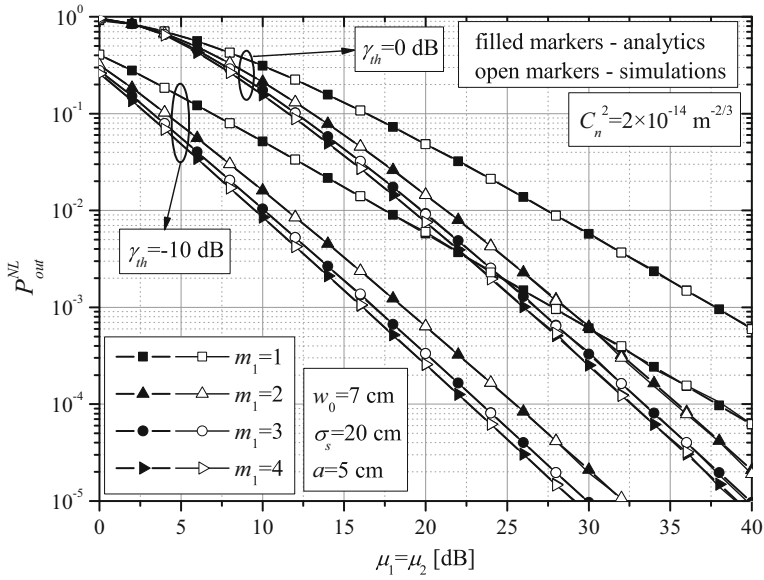
Fig. 2 Outage probability versus average electrical SNR over FSO link when relay suffers from noise for different values of jitter standard deviation

are manifested in the degradation of the system performance. In the range of low and moderate values of μ_2, the outage probability decreases, but for great values of μ_2, outage tends to a constant value. This outage floor cannot be decreased by further increasing average electrical SNR over the FSO link, but only by increasing the average SNR over RF link. The value of μ_2, when the outage floor appears, decreases with μ_1 and/or σ_s decreasing. In addition, the case when the pointing errors effect is negligible and the intensity fluctuations are caused only by the Gamma–Gamma turbulence is observed. One can notice overlapping of the curves corresponding to $\sigma_s = 10$ cm ($\sigma_s/a = 2$) and those when there is no misalignment fading.

Figure 3 plots the outage probability versus the average SNRs over both hops for different values of outage threshold and fading severity in NL system. As expected, outage probability decreases with decreasing γ_{th}. In addition, with increasing the parameter m_1, corresponding to decreasing fading severity, system has better outage performance. The worst performance exists for $m_1 = 1$, which corresponds to Rayleigh fading. The effect of fading severity on the outage performance is more pronounced when outage threshold is lower. For example, for $\mu_1 = \mu_2 = 20$ dB, by changing m_1 from 1 to 4, the outage probability decreases about 6.42 and 22.54 times in the case when γ_{th} is 0 and −10 dB, respectively. It is noticed that the outage floor does not appear in this case, since the outage probability dependence is presented in the function of the average SNR over both hops ($\mu_1 = \mu_2$), so both average SNRs increase simultaneously.

The effect of the number of interferers for different values of the average INR is presented in Fig. 4. The increasing of N reflects in worse system performance. The outage floor exists, and it takes different values for various number of CCIs. Also, the average INR effect on the outage floor is noticed. The influence of the number of interferers is more expressed while the average INR is greater. With decreasing the value of μ_I, the number of CCIs will be of a less importance on system performance. Further decreasing of μ_I, for

🖄 Springer

Fig. 3 Outage probability versus average SNR over both hops when relay suffers from noise for different values of fading severity
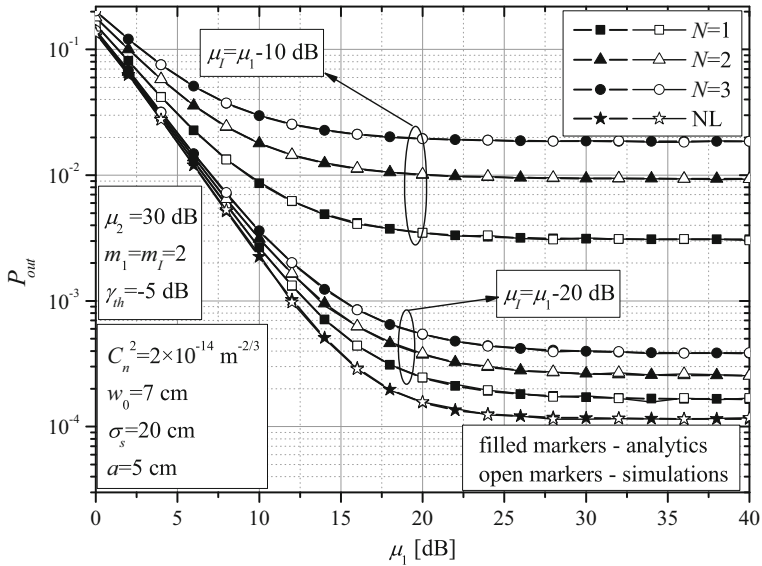
Fig. 4 Outage probability versus average SNR over RF link when relay suffers from multiple CCIs and noise

example $\mu_I = \mu_1 - 40$ dB, leads to the same system performance for any number of CCIs. The curve corresponding to this situation overlaps with one for the case of NL system (the results for this case are left out in Fig. 4. in order to avoid overcrowding of the curves). So,
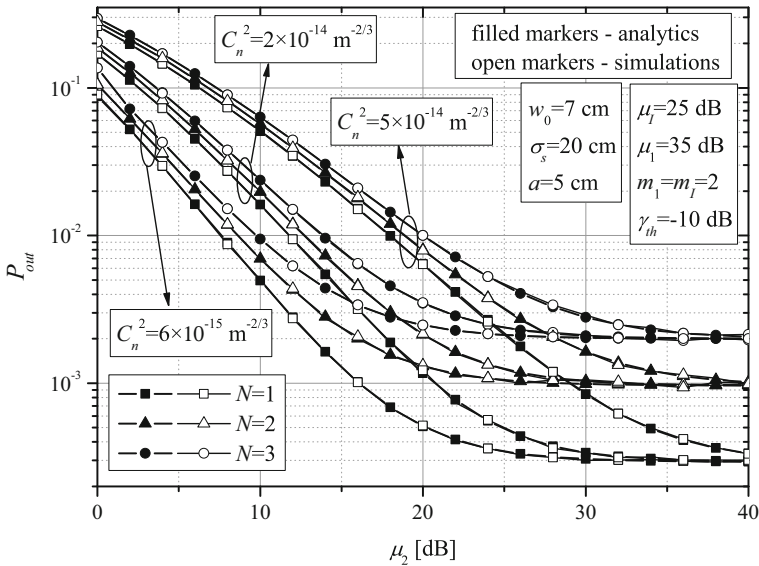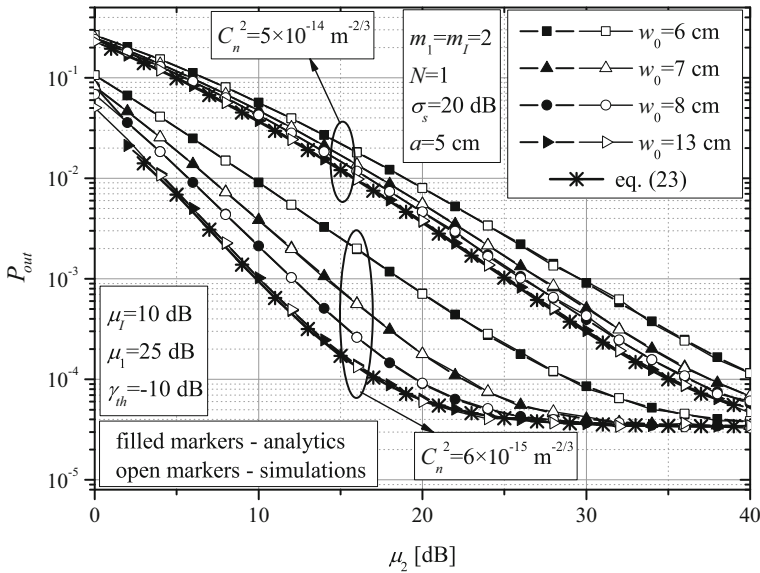
Fig. 5 Outage probability versus average electrical SNR over FSO link when relay suffers from multiple CCIs and noise in different turbulence conditions

when the power of the CCI is reducing, the CCIs will have no influence on the system performance, because the effect of the noise is dominant.

Figure 5 shows the influence of the number of CCIs on the outage performance in different turbulence conditions. As it is expected, system has better performance in weaker turbulence conditions and when number of CCIs is lower. Furthermore, the effect of the number of CCIs is more dominant in weak turbulence conditions, compared to the moderate and strong conditions. The existence of outage floor is also noted in this figure, appearing first in weak turbulence conditions.

The outage probability dependence on the average SNR over FSO hop for different values of the optical beam waist at the laser output, in weak and strong turbulence conditions, is presented in Fig. 6. The greater value of w_0 reflects in greater value of ξ, which corresponds to the case of non-pointing errors system. The overlapping of the curves for the system with $w_0 = 13$ cm and for the system under the influence of only Gamma–Gamma turbulence (Eq. 23), is noticed. With further increase of the optical beam waist, the outage probability performance remains closely the same. Also, the effect of different value of w_0 is more dominant in weak turbulence conditions compared to strong. When FSO link is affected by strong turbulence, the intensity fluctuations of the received signal are primarily caused by turbulence, so the pointing errors effect is of a less importance on system performance.

It can be noted that there is an agreement between analytical and simulation results presented in all figures.

Fig. 6 Outage probability versus average electrical SNR over FSO link when relay suffers from multiple CCIs and noise for different values of the optical beam waist at the laser output

5 Conclusion

In this paper, a dual-hop semi-blind AF mixed RF/FSO relaying channel has been analysed. Assuming the presence of both multiple CCIs and noise at the relay, the accurate closed-form expressions for the outage probability have been derived for Nakagami-m fading environment over RF link and the Gamma–Gamma turbulence with pointing errors over FSO link. The outage probability expression for the system with noise-limited $S - R$ link has been also derived, which can be simplified to the particular case of Rayleigh fading environment already reported. All numerical results have been verified by Monte Carlo simulations. The obtained formulae can be applied for estimating the outage probability dependence on the simultaneous effects of the fading severity, outage threshold, average SNRs of the both hops and average INR, as well as optical turbulence strength and pointing errors parameters. The numerical results have shown that there is an outage probability floor in the observed system. This irreducible outage probability is important system parameter and can be efficiently computed by the expressions derived here. The results have shown that effect of N is stronger in the regime of higher values of INR and weaker turbulence over FSO hop. In addition, the effects of photodetector displacement standard deviation could be strong for selected values of parameters.

6 Appendix A

The double integral in (20) consists of two independent integrals, i.e. $I = I_1 \times I_2$, where the first one, given by

$$I_1 = \int_0^\infty \gamma_2^{-i-1} e^{-\frac{m_1\gamma_{th}C_1}{\mu_1\gamma_2}} G_{1,3}^{3,0}\left(\alpha\beta\varepsilon\sqrt{\frac{\gamma_2}{\mu_2}}\,\middle|\,\begin{matrix}\xi^2+1\\\xi^2,\ \ \alpha,\ \ \beta\end{matrix}\right)d\gamma_2 \qquad (28)$$

can be solved as follows. The exponential function is expressed in terms of Meijer's G function by [22, Eq. (01.03.26.0004.01)], and afterwards transformed using [22, Eq. (07.34.16.0002.01)] as

$$e^{-\frac{m_1\gamma_{th}C_1}{\mu_1\gamma_2}} = G_{0,1}^{1,0}\left(\frac{m_1\gamma_{th}C_1}{\mu_1\gamma_2}\,\middle|\,\begin{matrix}-\\0\end{matrix}\right) = G_{1,0}^{0,1}\left(\frac{\mu_1\gamma_2}{m_1\gamma_{th}C_1}\,\middle|\,\begin{matrix}1\\-\end{matrix}\right) \qquad (29)$$

Using [22, Eq. (07.34.21.0013.01)] the integral I_1 can be expressed in the form

$$I_1 = \frac{2^{\alpha+\beta-2}}{\pi}\left(\frac{\mu_1}{m_1\gamma_{th}C_1}\right)^i G_{2,7}^{7,0}\left(\frac{\alpha^2\beta^2\varepsilon^2 m_1\gamma_{th}C_1}{16\mu_1\mu_2}\,\middle|\,\begin{matrix}\frac{\xi^2+1}{2},\ \frac{\xi^2+2}{2}\\\kappa_3\end{matrix}\right), \qquad (30)$$

where

$$\kappa_3 = \frac{\xi^2}{2},\ \ \frac{\xi^2+1}{2},\ \ \frac{\alpha}{2},\ \ \frac{\alpha+1}{2},\ \ \frac{\beta}{2},\ \ \frac{\beta+1}{2},\ \ i. \qquad (31)$$

The Meijer's G function in (30) can be re-written in a simpler form using following transformations. First, the permutations of the Meijer's G parameters are performed using [22, Eqs. (07.34.04.0003.01), (07.34.04.0004.01)]. Thereafter, the Meijer's G function is simplified by [22, Eq. (07.34.03.0002.01)], so the integral I_1 is given in the form

$$I_1 = \frac{2^{\alpha+\beta-2}}{\pi}\left(\frac{\mu_1}{m_1\gamma_{th}C_1}\right)^i G_{1,6}^{6,0}\left(\frac{\alpha^2\beta^2\varepsilon^2 m_1\gamma_{th}C_1}{16\mu_1\mu_2}\,\middle|\,\begin{matrix}\frac{\xi^2+2}{2}\\\kappa_1\end{matrix}\right), \qquad (32)$$

where κ_1 is previously defined by (22).

Using [21, Eq. (9.211.4)], the second integral I_2 is directly solved in the closed form

$$\begin{aligned}I_2 &= \int_0^\infty \gamma_I^{m_IN-1}(\gamma_I+1)^{k-i} e^{-\gamma_I\left(\frac{m_1}{\mu_1}\gamma_{th}+\frac{m_I}{\mu_I}\right)}d\gamma_I \\ &= \Gamma(m_IN)\mathrm{U}\left(m_IN, k-i+m_IN+1; \frac{m_I}{\mu_I}+\frac{m_1\gamma_{th}}{\mu_1}\right).\end{aligned} \qquad (33)$$

Combining previously derived expressions for I_1 and I_2 with (20) leads to (21).

7 Appendix B

In order to obtain the outage probability expression of the system without pointing errors effect, it is necessary to take a limit of derived Eq. (21) for $\xi \to \infty$. After applying [22, Eqs. (07.34.25.0007.01), (07.34.25.0006.01)], the outage probability of the system when intensity fluctuations are caused only by the Gamma–Gamma turbulence can be found as

$$P_{out,GG} = \lim_{\xi \to \infty} P_{out} = 1 - \frac{2^{\alpha+\beta-3}\xi^2}{\pi\Gamma(\alpha)\Gamma(\beta)} \left(\frac{m_I}{\mu_I}\right)^{m_I N} e^{-\frac{m_1\gamma_{th}}{\mu_1}}$$

$$\times \sum_{k=0}^{m_1-1} \sum_{i=0}^{k} \binom{k}{i} \frac{1}{k!} \left(\frac{m_1\gamma_{th}}{\mu_1}\right)^{k-i} U\left(m_I N, k-i+m_I N+1; \frac{m_I}{\mu_I}+\frac{m_1\gamma_{th}}{\mu_1}\right) \quad (34)$$

$$\times \lim_{\xi \to \infty} \xi^2 \frac{\Gamma\left(\frac{\xi^2}{2}\right)}{\Gamma\left(\frac{\xi^2+2}{2}\right)} G_{0,5}^{5,0}\left(\frac{\alpha^2\beta^2\varepsilon^2 m_1\gamma_{th}C_1\left(\xi^2+2\right)}{16\mu_1\mu_2\xi^2}\middle| \begin{matrix} - \\ \kappa_2 \end{matrix}\right).$$

where κ_2 is previously defined by (24). After applying [22, Eq. (06.05.16.0002.01)] and considering $\lim_{\xi \to \infty} \left(1 + 2/\xi^2\right) = 1$ and $\lim_{\xi \to \infty} \varepsilon^2 = \lim_{\xi \to \infty} \left(1 + 1/\xi^2\right)^2 = 1$, the outage probability for the system with the Gamma–Gamma distributed atmospheric turbulence over FSO link is derived in the form of (23).

References

1. Lee, E., Park, J., Han, D., & Yoon, G. (2011). Performance analysis of the asymmetric dual-hop relay transmission with mixed RF/FSO links. *IEEE Photonics Technology Letters*, 23(21), 1642–1644.
2. Ansari, I. S., Yilmaz, F. Y., & Alouini, M.-S. (2013). Impact of pointing errors on the performance of mixed RF/FSO dual-hop transmission systems. *IEEE Wireless Communications Letters*, 2(3), 351–354.
3. Samimi, H., & Uysal, M. (2013). End-to-end performance of mixed RF/FSO transmission systems. *IEEE Journal of Optical Communications and Networking*, 5(11), 1139–1144.
4. Popoola, W. O., Ghassemlooy, Z., Allen, J. I. H., Leitgeb, E., & Gao, S. (2008). Free-space optical communication employing subcarrier modulation and spatial diversity in atmospheric turbulence channel. *IET Optoelectronics*, 2(1), 16–23.
5. Samimi, H., & Azmi, P. S. (2011). Performance analysis of adaptive subcarrier intensity-modulated free-space optical systems. *IET Optoelectronics*, 5(4), 168–174.
6. Popoola, W. O., & Ghassemlooy, Z. (2009). BPSK subcarrier intensity modulated free-space optical communications in atmospheric turbulence. *Journal of Lightwave Technology*, 27(8), 967–973.
7. Simon, M. K., & Alouni, M.-S. (2004). *Digital communication over fading channels* (2nd ed.). New York: Wiley.
8. Ghassemlooy, Z., & Popoola, W. O. (2013). *Optical wireless communications: System and channel modelling with MATLAB*. New York: CRC Press.
9. Andrews, L. C., & Philips, R. N. (2005). *Laser beam propagation through random media* (2nd ed.). Bellingham: Washington:Spie Press.
10. Al-Habash, M. A., Andrews, L. C., & Philips, R. N. (2011). Mathematical model for the irradiance probability density function of a laser beam propagating through turbulent media. *Optical Engineering*, 40(8), 1554–1562.
11. Nistazakis, H. E., Tsiftsis, T. A., & Tombras, G. S. (2009). Performance analysis of free-space optical communication systems over atmospheric turbulence channels. *IET Communications*, 3(8), 402–1409.
12. Farid, A. A., & Hranilovic, S. (2007). Outage capacity optimization for free space optical links with pointing errors. *Journal of Lightwave Technology*, 25(7), 1702–1710.
13. Farid, A. A., & Hranilovic, S. (2011). Outage capacity for MISO intensity-modulated free-space optical links with misalignment. *IEEE Journal of Optical Communications and Networking*, 3(10), 780–789.
14. Sandalidis, H. G., Tsiftsis, T. A., & Karagiannidis, G. K. (2009). Optical wireless communications with heterodyne detection over turbulence channels with pointing errors. *Journal of Lightwave Technology*, 27(20), 4440–4445.
15. Gappmair, W. (2011). Further results on the capacity of free-space optical channels in turbulent atmosphere. *IET Communications*, 5(9), 1262–1267.
16. Hasna, M. O., Alouini, M.-S., Bastami, A., & Ebbini, E. S. (2003). Performance analysis of cellular mobile systems with successive co-channel interference cancellation. *IEEE Transactions on Wireless Communications*, 2(1), 29–40.

17. Alouini, M.-S., & Goldsmith, A. J. (1999). Area spectral efficiency of cellular mobile radio systems. *IEEE Transactions on Vehicular Communications*, *48*(4), 1047–1066.
18. Xu, F., Khalighi, M.-A., & Bourennane, (2011). Impact of different noise sources on the performance of PIN- and APD-based FSO receivers. In *11th international conference on telecommunications (ConTEL 2011)* (pp. 211–218), Graz, Austria.
19. Suraweera, H. A., Michalopoulos, D. S., Schober, R., Karagiannidis, G. K., & Nallanathan, A. (2011). Fixed gain amplify-and-forward relaying with co-channel interference. *IEEE International Conference on Communications (ICC)*, *2011*, 1–6.
20. Xia, M., Xing, C., Wu, Y. C., & Assa, S. (2011). Exact performance analysis of dual-hop semi-blind AF relaying over arbitrary Nakagami-m fading channels. *IEEE Transactions on Wireless Communications*, *10*(10), 3449–3459.
21. Gradshteyn, I. S., & Ryzhik, I. M. (2000). *Table of integrals, series, and products* (6th ed.). New York: Academic.
22. The Wolfarm Functions Site. (2008). (Online) Available: http://functions.wolfarm.com
23. Luong, D. A., Thang, T. C., & Pham, A. T. (2013). Effect of avalanche photodiode and thermal noises on the performance of binary phase-shift keying-subcarrier-intensity modulation/free-space optical systems over turbulence channels. *IET Communications*, *7*(6), 738–744.

Milica I. Petkovic was born in Knjazevac, Serbia, in 1986. She received her M.Sc. and Ph.D. degrees in electrical engineering from the Faculty of Electronic Engineering, University of Nis, Serbia, in 2010, and 2016, respectively. Currently, she is a Research Assistant at the Department of Telecommunications, Faculty of Electronic Engineering, University of Nis, Serbia. Her research interests include communication theory, wireless and optical communication systems, application of different modulation techniques and modeling of fading channels. Her Ph.D degree is in the field of free-space optical systems. She has published several papers on the above subjects.

Aleksandra M. Cvetkovic was born in Nis, Serbia. She received B.S. M.S., and Ph.D. degrees in electrical engineering from the Faculty of Electronic Engineering, University of Nis, Serbia, in 2001, 2007. and 2013, respectively. She is currently working at the Faculty of Electronic Engineering, Nis, Serbia, as an Assistant. Her research interests include wireless communication theory, cooperative communication and free space optical system. Other areas of research include statistical characterization and modeling of fading channels and performance analysis of multi user wireless systems subject to interference. She has published several papers–on the above subjects.

Goran T. Djordjevic was born in Nis, Serbia. He received his B.S., M.S., and Ph.D. degrees in electrical engineering from the Faculty of Electronic Engineering, University of Nis, Serbia, in 1996, 1999 and 2005, respectively. His area of interest is communication theory and applications in satellite, wireless and optical communication systems. His current research interests include application of different modulation formats and error control codes in free space optical systems, modeling and simulation of fading channels, synchronization problems. Currently he is an Associate Professor at the Department of Telecommunications, Faculty of Electronic Engineering, University of Nis, Serbia. He teaches courses of Communication Theory, Modeling and Simulation of Communication Systems, Information Theory and Satellite Communications.

George K. Karagiannidis (M'96-SM'03-F'14) was born in Pithagorion, Samos Island, Greece. He received the University Diploma (5 years) and PhD degree, both in electrical and computer engineering from the University of Patras, in 1987 and 1999, respectively. From 2000 to 2004, he was a Senior Researcher at the Institute for Space Applications and Remote Sensing, National Observatory of Athens, Greece. In June 2004, he joined the faculty of Aristotle University of Thessaloniki, Greece where he is currently Professor in the Electrical & Computer Engineering Dept. and Director of Digital Telecommunications Systems and Networks Laboratory. He is also Honorary Professor at South West Jiaotong University, Chengdu, China. His research interests are in the broad area of Digital Communications Systems and Signal processing, with emphasis on Wireless Communications, Optical Wireless Communications, Wireless Power Transfer and Applications, Molecular and Nanoscale Communications, Stochastic Processes in Biology and Wireless Security. He is the author or co-author of more than 400 technical papers published in scientific journals and presented at international conferences. He is also author of the Greek edition of a book on "Telecommunications Systems" and co-author of the book "Advanced Optical Wireless Communications Systems", Cambridge Publications, 2012. Dr. Karagiannidis has been involved as General Chair, Technical Program Chair and member of Technical Program Committees in several IEEE and non-IEEE conferences. In the past, he was Editor in IEEE Transactions on Communications, Senior Editor of IEEE Communications Letters, Editor of the EURASIP Journal of Wireless Communications & Networks and several times Guest Editor in IEEE Selected Areas in Communications. From 2012 to 2015 he was the Editor-in Chief of IEEE Communications Letters. Dr. Karagiannidis is IEEE Fellow and one of the highly-cited authors across all areas of Electrical Engineering, recognized as 2015 and 2016 Thomson Reuters highly-cited researcher.